Article

The potential of high-frequency profiling to assess vertical and seasonal patterns of phytoplankton dynamics in lakes: an extension of the Plankton Ecology Group (PEG) model

Jennifer A. Brentrup,[1]* Craig E. Williamson,[1] William Colom-Montero,[2] Werner Eckert,[3] Elvira de Eyto,[4] Hans-Peter Grossart,[5,6] Yannick Huot,[7] Peter D.F. Isles,[8] Lesley B. Knoll,[9] Taylor H. Leach,[1] Chris G. McBride,[10] Don Pierson,[11] Francesco Pomati,[12] Jordan S. Read,[13] Kevin C. Rose,[14] Nihar R. Samal,[15] Peter A. Staehr,[16] and Luke A. Winslow[13]

[1] *Department of Biology, Miami University, Oxford, OH, USA*
[2] *Erken Laboratory, Department of Ecology and Genetics, EBC, Uppsala University, Norrtälje, Sweden*
[3] *Israel Oceanographic and Limnological Research, The Yigal Allon Kinneret Limnological Laboratory, Migdal, Israel*
[4] *Marine Institute, Furnace, Newport, Co. Mayo, Ireland*
[5] *Leibniz Institute of Freshwater Ecology and Inland Fisheries (IGB), Department Experimental Limnology, Stechlin, Germany*
[6] *Potsdam University, Institute for Biochemistry and Biology Potsdam University, Potsdam, Germany*
[7] *Département de géomatique appliquée, University of Sherbrooke, Sherbrooke, Québec, Canada*
[8] *Rubenstein School of Environment and Natural Resources, University of Vermont, Burlington, VT, USA*
[9] *Itasca Biological Station, University of Minnesota, Lake Itasca, MN, USA*
[10] *Environmental Research Institute, University of Waikato, Waikato, New Zealand*
[11] *Department of Limnology, Institute of Ecology and Genetics, EBC, Uppsala University, Uppsala, Sweden*
[12] *Department of Aquatic Ecology, Eawag: Swiss Federal Institute of Aquatic Science and Technology, Dübendorf, Switzerland*
[13] *US Geological Survey, Center for Integrated Data Analytics, Middleton, WI, USA*
[14] *Department of Biological Sciences, Rensselaer Polytechnic Institute, Troy, NY, USA*
[15] *Earth Systems Research Center, University of New Hampshire, Durham, NH, USA*
[16] *Department of Bioscience, Aarhus University, Roskilde, Denmark*
* Corresponding author: brentrja@miamioh.edu

Received 11 May 2015; accepted 26 January 2016; published 2 November 2016

Abstract

The use of high-frequency sensors on profiling buoys to investigate physical, chemical, and biological processes in lakes is increasing rapidly. Profiling buoys with automated winches and sensors that collect high-frequency chlorophyll fluorescence (ChlF) profiles in 11 lakes in the Global Lake Ecological Observatory Network (GLEON) allowed the study of the vertical and temporal distribution of ChlF, including the formation of subsurface chlorophyll maxima (SSCM). The effectiveness of 3 methods for sampling phytoplankton distributions in lakes, including (1) manual profiles, (2) single-depth buoys, and (3) profiling buoys were assessed. High-frequency ChlF surface data and profiles were compared to predictions from the Plankton Ecology Group (PEG) model. The depth-integrated ChlF dynamics measured by the profiling buoy data revealed a greater complexity that neither conventional sampling nor the generalized PEG model captured. Conventional sampling techniques would have missed SSCM in 7 of 11 study lakes. Although surface-only ChlF data underestimated average water column ChlF, at times by nearly 2-fold in 4 of the lakes, overall there was a remarkable similarity between surface and mean water column data. Contrary to the PEG model's proposed negligible role for physical control of phytoplankton during the growing season, thermal structure and light availability were closely associated with ChlF seasonal depth distribution. Thus, an extension of the PEG model is proposed, with a new conceptual framework that explicitly includes physical metrics to better predict SSCM formation in lakes and highlight when profiling buoys are especially informative.

Key words: chlorophyll fluorescence, Global Lake Ecological Observatory Network (GLEON), high-frequency sensors, PEG model, phytoplankton, profiling buoys, subsurface chlorophyll maximum

DOI: 10.5268/IW-6.4.890

Inland Waters (2016) **6**, pp.565–580

The work featured in this special issue of Inland Waters was partially supported by NSF award EF1137327

Introduction

Subsurface chlorophyll maxima (SSCM) are common and widespread in both freshwater and marine ecosystems (Fee 1976, Huisman et al. 2006, Hamilton et al. 2010, Beisner and Longhi 2013, Cullen 2015). Little is known, however, about the dynamics of these chlorophyll layers and their influence on overall productivity in lakes. Understanding the impact of SSCM on lake ecology is hindered by the ability to achieve adequate spatial and temporal sampling resolution. In some cases, net primary production at the SSCM can account for as much as 72% of the productivity on an areal basis in oligotrophic lakes (Moll and Stoermer 1982). Sub-epilimnetic phytoplankton production in transparent, low-nutrient lakes can be important for higher trophic levels because it may represent a high-quality food source for zooplankton (Williamson et al. 1996, Matthews and Mazumder 2006, Francis et al. 2011) as well as a nutritional source for benthic filter feeders (Malkin et al. 2012). Inland waters are experiencing increasing pressures ranging from shifts in land use and land cover within their catchment to climate change and consequent increases in air temperature, drought, and extreme precipitation events (Grimm et al. 2013, Hayes et al. 2015). Many of these changes lead to declining water transparency that in turn may shift or inhibit the formation of SSCM layers. Increasing nutrient loads and warming air and water temperatures contribute to cultural eutrophication of inland and coastal waters, which may increase the formation of surface blooms of toxic cyanobacteria and other algae, with many negative ecosystem consequences (Carpenter et al. 1998, Dodds et al. 2009, Brookes and Carey 2011, Taranu et al. 2015).

A major challenge in aquatic ecosystem science is to accurately characterize the spatial and temporal dynamics of subsurface phytoplankton blooms and their impact on lake water quality, productivity, and food web ecology. Recent advances in environmental sensors and observation platforms are rapidly increasing our ability to resolve both temporal and vertical dynamics of physical, chemical, and biological factors in lakes, providing new insights into these understudied subsurface features. Challenges still arise with these new methods, however, because chlorophyll-based observations have the potential to overestimate phytoplankton biomass. For instance, although chlorophyll *a* (Chl-*a*) measurements from water sample extracts or *in situ* fluorescence are often used to assess phytoplankton dynamics, chlorophyll to biomass ratios increase under the lower light and higher nutrient conditions of the SSCM environment (Geider et al. 1998, Fennel and Boss 2003). Non-photochemical quenching of chlorophyll fluorescence (ChlF) can also complicate the interpretation of fluorescence profiles made during the day (Huot and Babin 2010). When phytoplankton are exposed to high irradiance, a greater fraction of the absorbed energy is released as heat, reducing the quantum yield of fluorescence, and thereby the measured ChlF per unit of Chl-*a*, leading to a reduced estimate of Chl-*a* relative to dark regulated cells (e.g., Serra et al. 2009, Huot and Babin 2010, Proctor and Roesler 2010). Despite these limitations, chlorophyll remains one of the most effective proxies to assess the complex spatial and temporal dynamics of SSCM, which are observed not only in lakes but also in many areas of the ocean (Cullen 2015). Buoy-based ChlF measurements have the additional advantage of collecting data remotely at night, leading to more stable and accurate chlorophyll measurements from *in situ* fluorometers than with manual daytime sampling.

Early research on SSCM by Fee (1976) provided clear evidence for the need to collect continuous profiles instead of sampling over discrete depths. Fee compared discrete samples and manual ChlF profiles in 6 lakes of the Experimental Lakes Area in northwestern Ontario to show that whole lake chlorophyll estimates from discrete samples would have missed the chlorophyll peak entirely and only captured 40% of the total mass of chlorophyll in a lake (1976). Recently, coupled hydrodynamic and ecological models have taken a more mechanistic approach to understanding the drivers of phytoplankton vertical positioning in the water column (Mellard et al. 2011, White and Matsumoto 2012, Hamilton et al. 2015), but such models require high resolution data to validate the variability observed. Advanced methods that capture short-term vertical phytoplankton dynamics are necessary because the maximum specific growth rate of phytoplankton can be on the order of 0.1–0.86 d^{-1} (Reynolds 2006), and phytoplankton blooms can form and dissipate within a few days. The phytoplankton species that commonly form SSCM consist of mobile species adapted to live in low-light conditions, such as *Cryptomonas* spp., *Dinobryon* spp., *Gymnodinium* spp., *Chrysosphaerella* spp., and *Synura* spp. (Fee 1976, Barbiero and Tuchman 2004, Reynolds 2006). Some phytoplankton species (i.e., phytoflagellates) also show daily migrations, and vertical migration rates can range from <1 to 20 m d^{-1} or even as high as 90 m d^{-1} for some species of *Microcystis* (Reynolds and Walsby 1975). Therefore, to describe the frequency and intensity of phytoplankton blooms, an estimated minimum sample frequency of 4–6 times per week would be needed (Pomati et al. 2011), but even higher frequency sampling of multiple times per day would be necessary to capture their vertical migrations.

These short-term dynamics can have far-reaching effects that influence the seasonal structure and phenology of phytoplankton distributions. Manual profiles once a

 DOI: 10.5268/IW-6.4.890

week or once every 2 weeks will be insufficient to capture fine-scale vertical dynamics, and sensors deployed at the lake surface will miss variation in ChlF below the surface mixed layer that occurs during thermally stratified periods. The phenology of SSCM are one feature in lakes that can be missed with surface only sampling, which can lead to large underestimates of Chl-*a* because the Chl-*a* concentration in deep layers can be 1.5–2.5 times greater than in surface layers (Barbiero and Tuchman 2004). High-frequency temporal and vertical measurements are therefore needed to provide a more thorough assessment of the seasonal changes in phytoplankton dynamics and the drivers of planktonic succession across temporal scales ranging from hours to months.

The Global Lake Ecological Observatory Network (GLEON) has brought scientists together with the common goal of using high-frequency sensor data collected on buoys deployed in lakes around the world to improve the understanding of lake functions (Weathers et al. 2013). Although many GLEON sites use stationary buoys to deploy sensors at a single depth, recent technological advancements have made it feasible to collect high temporal and depth-distributed data with profiling buoys. Profiling buoys have commonly been used for oceanographic research (Prairie et al. 2011, Mignot et al. 2014), but their use in limnology is more recent, and few studies have been published to date (Pomati et al. 2011, Staehr et al. 2012, Obrador et al. 2014). Studies by Staehr et al. (2012) and Obrador et al. (2014) used profiling buoys to investigate vertical heterogeneity in metabolism estimates, and Pomati et al. (2011) coupled high-frequency profiling with flow-cytometry to understand the drivers of diversity and dynamic processes in phytoplankton communities in one lake. High-frequency profiling captured an environmental disturbance that led to decreased functional diversity and a period of cyanobacterial dominance that would have been missed with traditional limnological methods (Pomati et al. 2011). Recent advances in autonomous and Lagrangian platforms and sensors (ALPS) were summarized in a special issue by Dickey et al. (2008); however, only one paper in the issue included a lake study with an autonomous vertical profiler (Caron et al. 2008). The authors investigated micro-scale dynamics of phytoplankton and found high spatial and temporal heterogeneity in ChlF, potentially due to vertical mixing and migratory behavior of phytoplankton (Caron et al. 2008). Previous studies have focused on a single or a few nearby lakes, but the large vertical heterogeneity in phytoplankton dynamics observed in these profiling buoy studies highlights the need for further research examining subsurface ChlF layers at high-resolution temporal and vertical scales across a global set of lakes. Profiling buoys also have the added benefit of collecting data over the entire ice-free season or year-round, so seasonal changes in phytoplankton dynamics can be examined in relation to existing conceptual models.

In 1986, the Plankton Ecology Group (PEG) developed a conceptual model to explain the seasonal patterns of change in phytoplankton biomass, leading to one of the most cited papers in limnology (Sommer et al. 1986). This conceptual model was revisited by the same group 26 years later, and although recent research on multiple factors including limitation by parasites, food quality, predators, and climate change were found to explain some of the changes in species composition, the fundamental seasonal patterns of phytoplankton dynamics remained unchanged (Sommer et al. 2012, De Senerpont Domis et al. 2013). Although neither the original PEG model nor subsequent papers stated at what depth data were collected to inform the model, the predictions were likely based on periodic, epilimnetic samples. Because of the widespread occurrence of SSCM in many lakes, more explicit analysis of phytoplankton abundance throughout the water column could strengthen and improve the PEG model.

Despite early work identifying the importance of physical factors for SSCM in lakes (e.g., Fee 1976, Abott et al. 1984), the PEG model hypothesizes that physical control on phytoplankton is low throughout the growing season (Sommer et al. 1986, 2012). The model focuses on the predominance of biological events regulating phytoplankton dynamics, with physical factors thought to be important only during the beginning and end of spring and fall. Physical factors, specifically light and temperature, have previously been shown to be important regulators of the depth of the SSCM in aquatic ecosystems (Fee 1976, Cullen 1982, Abbott et al. 1984, Hamilton et al. 2010, Beisner and Longhi 2013, Jobin and Beisner 2014). Thermal stratification is often considered a prerequisite for SSCM development in lakes (Jobin and Beisner 2014); however, once thermal stratification is in place, the euphotic depth is often highly correlated with the depth of the SSCM (Fee 1976, Hamilton et al. 2010).

Here, we examined the potential for *in situ* fluorometers on automated profiling buoys to more fully resolve the temporal and vertical resolution of phytoplankton using ChlF as a proxy. Classical manual sampling of phytoplankton in lakes can now be augmented with sensors used (1) for manual profiles, (2) on single depth automated buoys, and more recently (3) with automated buoys that provide vertical profiles of the water column. Specifically, we asked: how can high-resolution temporal and vertical ChlF data collected with fluorometers on profiling buoys add to our understanding of seasonal patterns of phytoplankton dynamics and extend the PEG model? Our study encompassed 11 lakes across the globe that span a gradient of trophic status. We compared high-frequency ChlF data

Table 1. Summary characteristics of the 11 lakes used in the analysis. Epilimnetic chlorophyll (Chl-*a*), 1% PAR depth, and Secchi depth are June–August averages for the profiling buoy deployment year, except for Lake Rotoehu data, which are a December–February average. Lakes are sorted by trophic status according to epilimnetic Chl-*a*.

Lake	Country	Lat.	Long.	Year	Lake area (km^2)	Max depth (m)	Lake mixing status[+]	Trophic status[#]	Epilimnetic Chl-*a* ($\mu g\ L^{-1}$) ± SD	1% PAR depth (m) ± SD	Secchi depth (m) ± SD
Lacawac	USA	41°22′N	75°17′W	2014	0.2	13	D	O, DY	1.5 ± 0.7	5.8 ± 0.6	3.2 ± 0.3
Crystal	USA	46°N	89°35′W	2014	0.34	20.4	D	O	1.6 ± 0.6	14.9 ± 0.9	7.1 ±1.3
Montjoie	Canada	45°24′N	72°6′W	2013	3.29	22.2	D	O	2.3 ± 0.9	7.4 ± 0.6	3.2 ± 0.5
Furnace	Ireland	53°55′N	9°34′W	2013	1.41	21	ME	O, DY	2.3 ± 0.9	4.7[c]	1.8
Ashokan	USA	41°56′N	74°13′W	2011	12.2	56.4	D	O	2.6 ± 0.8	7.3 ± 2.1	NA
Erken	Sweden	59°51′N	18°37′E	2014	24.2	21	D	M	4.9 ± 4.0	8.8[c]	3.9 ± 0.9
Rotoehu	NZ*	38°1′S	176° 32′E	2014	8.1	13.5	P	M	5.1 ± 2.3	7.7 ± 1.8[c]	3.4 ± 0.8
Bure	Denmark	55°50′N	12°13′E	2012	0.76	10.8	P	M	6.3 ± 3.6	7.2 ± 1.3	3.8 ± 1.0
Greifensee	SWZ**	47°21′N	8°41′E	2013	8.5	32	MO	E	9.3 ± 4.9	8.7 ± 3.3	NA
Mendota	USA	43°5′N	89°24′W	2010	39.4	26	D	E	9.9 ± 5.8	7.9[c]	3.5 ± 2.4
Kinneret	Israel	32°50′N	35°35′E	2014	170	42	MO	E	17.6 ± 13.5	10.3 ± 1.7	2.9 ± 0.5

* New Zealand, ** Switzerland; [+] D = dimictic, ME = meromictic, P = polymictic, MO = monomictic; [#] O = oligotrophic, M = mesotrophic, DY = dystrophic, E = eutrophic; [c] 1% PAR depth estimated by multiplying Secchi depth by 2.25

collected at the lake surface, as well as averaged over the water column, to the generalized PEG model for eutrophic and oligotrophic lakes. We then assessed the advantages and limitations of the 3 sampling methods in resolving the seasonal patterns of phytoplankton dynamics. Finally, to examine the role of physical control on SSCM, we used high-frequency profiling buoy data from 3 representative study lakes (small, oligotrophic Crystal; moderate-sized, oligo-mesotrophic Montjoie; and larger, eutrophic Greifensee; Table 1) to produce depth versus time isopleths of ChlF that enable visualization of the relationship between important physical characteristics of the lakes (i.e., euphotic zone as well as the upper and lower metalimnion boundaries) and phytoplankton dynamics.

Methods

Study sites

High-frequency temporal and spatial ChlF data from automated profiling buoys were used to assess seasonal phytoplankton dynamics in 9 temperate and 2 subtropical lakes. All sites contribute data to GLEON, and all but 1 lake (Rotoehu, New Zealand) are in the Northern Hemisphere. Of the study lakes 5 were oligotrophic, 3 mesotrophic, and 3 eutrophic, with mean summer (Jun–Aug) epilimnetic Chl-*a* concentrations averaging 1.5–2.6, 4.9–6.3, and 9.3–17.6 $\mu g\ L^{-1}$, respectively (Table 1). The study lakes cover a wide range of mixing regimes including 6 dimictic, 2 polymictic, 2 monomictic, and Furnace, a meromictic, coastal brackish lake that has not mixed completely since 1995 (Cassina et al. 2013). Furnace also experiences tidal influences and blooms of marine or brackish water phytoplankton species following especially high tides (E. de Eyto, Marine Institute, unpubl. data). The lakes range in area from 0.2 km^2 for Lacawac to 170 km^2 for Kinneret, and maximum depths range from 10.8 m in Bure to 56.4 m in the west basin of Ashokan Reservoir. A single year of profiling buoy data from each lake was analyzed for this study, primarily from 2013 or 2014 (Table 1).

Profiling buoy and sensor information

Profiling buoys were deployed during the ice-free season (ranging from Apr to Nov) for temperate lakes or year-round where weather conditions allowed. The minimum time period of data collected was 3 months. The type of profiling buoy used was lake-specific and ranged from commercially available systems to individually designed automated profiling moorings (Fig. 1). Profiling buoys were typically powered by solar panels and rechargeable batteries. The number of vertical profiles collected per day varied from 4 to 48 (Table 2). The depth resolution of the profiles spanned a wide range with near continuous profiles at 0.03 m intervals to the more common approach of sampling at 1 m resolution from the lake surface to near the lake bottom (Table 2).

Each of the study lakes has a unique profiling system, and a suite of different sensors is often profiled together with a variety of methods used to transmit the data, including radio, cellular, and Bluetooth communication systems. When profiling, a "dwell time" is often used to allow slow response sensors (e.g., pH and dissolved oxygen) time to stabilize. Dwell times for the profiling buoys in this study ranged from near continuous (1 s) to

 DOI: 10.5268/IW-6.4.890

Table 2. Profiling buoy and chlorophyll fluorometer sensor manufacturer information. Profiling depth range represents the range of depths sampled by the profiling buoy, and the resolution in parentheses corresponds to the sample interval at which each of the readings was taken throughout this depth range. Dwell time corresponds to the duration (s) the profiler was stationary at each depth before a reading was taken. Company information for the sensor manufacturers is included below the table.

Lake	Number of profiles per day	Profile depth range and sampling interval (m)	Chlorophyll fluorometer sensor manufacturer	Dwell time (s)
Lacawac	4	0.5, 1–12 (1)	Turner Designs Cyclops-7[a]	360
Crystal	24	1–18 (1)	Turner Designs Cyclops-7	420
Montjoie	8–24*	0.3–14.5 (0.03)	Wetlabs ECO[b]	1
Furnace	4	0.1–11.7 (0.17)	Datasonde DX5[c]	120
Ashokan	4	0–33 (1)	YSI 6600 V2[d]	360
Erken	4	1–11 (1)	YSI 6600 V2 & YSI EXO2	60
Rotoehu	12	0.5–8.5 (0.5)	Turner Designs Cyclops-7	60
Bure	48	0.5, 1–9 (1)	YSI 6600 V2	120
Greifensee	12	1.4–17 (0.1)	Chelsea Technologies TriLux[e]	1
Mendota	12	2–18 (1)	YSI 6600 V2	420
Kinneret	2–4	0–39 (0.5)	Turner Designs Cyclops-7	30

* Profiles in Montjoie were every 3 h from 13 June to 11 July; every 2 h from 11 July to 15 August; and every 1 h from 15 to 25 August 2013; [a] Sunnyvale, CA, USA; [b] Philomath, OR, USA; [c] Portland, OR, USA; [d] Yellow Springs, OH, USA; [e] West Molesey, Surrey, UK

Fig. 1. Images of profiling buoys from 11 GLEON member study lakes. Profiling buoys, arranged in alphabetical order starting from the top left-hand corner and left to right are as follows: Ashokan, Bure, Crystal, Erken, Furnace, Greifensee, Kinneret, Lacawac, Mendota, Montjoie, and Rotoehu. Photo credits: Ashokan: Perri Paul and Tom Mills, NYC DEP; Bure: Peter Staehr; Crystal: Kevin Rose; Erken: William Colom-Montero; Furnace: Elizabeth Ryder; Kinneret: Werner Eckert; Lacawac: Lesley Knoll; Mendota: Luke Winslow; Montjoie: Yannick Huot; and Rotoehu: Chris McBride.

7 min, but because of the fast response time (<1 s) of most ChlF, irradiance, and water temperature sensors used in this analysis, differences in dwell time between the lakes are likely less important (Table 2). Commercially available ChlF sensors from a range of different manufacturers were deployed on the profiling buoys (Table 2). The minimum chlorophyll detection limit of all of the sensors was <0.1 μg L^{-1}. Wipers were used on most of the ChlF sensors to prevent biofouling, or sensors were cleaned manually once every 2 weeks; data were quality-control checked, and any erroneous readings were removed.

In addition to ChlF data, temperature and photosynthetically active radiation (PAR) data were used from 3 of the lakes. In Montjoie, temperature data were collected using a Multiparameter 600R sonde (YSI, Ohio, USA; 0.25 Hz). The 600R temperature sensor has a slower response time than the ChlF sensors, and results are considered to be a weighted average of the last ~40 cm. Irradiance data were measured with a Hyperspectral irradiance sensor (HyperOCR, Satlantic, Canada) every 3 nm in the visible wavelength range (400–700 nm). In Crystal, automated irradiance buoy profiles were not collected, so manual profiles collected with a LiCor PAR sensor (Lincoln, NE, USA) and a profiling ultraviolet (PUV) radiometer (PAR channel 400–700 nm; Biospherical Instruments Inc., CA, USA) were used instead. Temperature data were collected on the profiling buoy with a Hydrolab temperature sensor (CO, USA). Lastly, in Greifensee, automated irradiance profiles were also collected with a LiCor sensor, and temperature data were measured with an Ocean Seven 316Plus CTD (O7) multiparameter probe (Idronaut, Brugherio, Italy).

Chlorophyll fluorescence data analysis

Because of the variability in sensor manufacturers (Table 2) and the lack of intercalibration among sensors, analyses herein focus on relative changes in ChlF over depth and time within each lake as well as how these relative patterns vary among lakes. No comparisons were made between the absolute magnitude of the ChlF signal among lakes. Relationships between ChlF data and extracted Chl-*a* concentrations from water samples also vary widely and are specific to sensor type, lake, and time period as well as seasonal changes in light, nutrients, water temperature, and phytoplankton community composition (Cullen 1982). Therefore, no attempt was made to convert raw ChlF signals to Chl-*a* extraction equivalent concentrations except for Montjoie, where factory calibrations were used to provide an estimate of Chl-*a* concentrations. ChlF data were used as a proxy of phytoplankton biomass, with a focus on examining the rates of change over depth and time to provide a rapid, sensitive, and nonintrusive way to assess the relative amount of phytoplankton abundance present from automated profiles (Cullen 1982, Huot and Babin 2010).

For the analysis of vertical ChlF profiles, temperature corrections were not applied to the ChlF data because no appropriate method for applying a temperature correction to *in vivo* fluorescence data exists. To avoid reduced ChlF values associated with non-photochemical quenching (NPQ, discussed later), only nighttime data were used for all analyses except one lake. In Kinneret, a nighttime profile was used whenever possible, but these were not consistently taken at the beginning of the study period, so midday profiles were used (Jan and Feb only). Kinneret is also one of the least transparent lakes in this study, and the impact of NPQ is likely restricted to the lake surface. Nighttime was defined as between 2200 and 0400 h local time for each lake. Midnight profiles were used unless unavailable, in which case the next closest profile in time was used.

NPQ often occurs at higher irradiance, so shallower surface waters are more susceptible, although the effect may extend deeper in transparent waters. To assess the potential importance of NPQ, daily ChlF profiles collected at noon in Crystal were subtracted from daily ChlF profiles collected at midnight. The greatest difference between the midnight and noon data was evident in the top 5 m of the water column in early May and extended down to 10 m in late May as the 1% PAR depth increased from 11 to 15 m (Fig. 2). Noon ChlF values at 1 m were as much as 5 relative fluorescence units (RFU) lower than the corresponding midnight ChlF values (Fig. 2).

To compare seasonal patterns in ChlF data from the profiling buoys with the PEG model (Sommer et al. 1986, 2012), ChlF data from the range of years in this study were standardized to the day of the year irrespective of the actual data collection year. The seasonal time scale for Rotoehu in the Southern Hemisphere was shifted by 6 months to match the seasonal patterns of the Northern Hemisphere. A LOESS smoothing procedure was applied to a daily time series of surface data and mean water column ChlF data collected at night, and the data were normalized to the seasonal maximum of the smoothed data. Surface readings ranged in depth from 0 to 2 m, and the shallowest reading with the least amount of missing data for each lake was used. These normalized data were scaled to a maximum value of 100 for eutrophic and mesotrophic lakes and 50 for oligotrophic lakes to be consistent with the presentation of the patterns in PEG model publications (Sommer et al. 1986, 2012).

The original PEG model line redrawn from figure 6 in Sommer et al. (1986) was superimposed on data from each of the profiling buoys. Because no time scale was provided on the original PEG model, the first low point on

 DOI: 10.5268/IW-6.4.890

the PEG time series was identified as the spring clear-water phase and used as a reference point to align the conceptual model to the buoy time series data based on studies identifying when the peak of the phytoplankton minimum occurs (Lampert et al. 1986, Sommer et al. 1986). In eutrophic lakes, the clear-water phase typically occurs in mid-May (Lampert et al. 1986), immediately after the spring phytoplankton peak, and lasts no longer than 1 month (Sommer et al. 1986). For mesotrophic and oligotrophic lakes, the clear-water phase occurs later (around mid-Jun) and extends further into the summer (Sommer et al. 1986, Williamson et al. 2007, Dröscher et al. 2009). Differences in the timing of the spring clear-water phase among lakes resulted in adjustment of the PEG model line accordingly to best match the profiling buoy data. Only relative differences are described here due to the conceptual nature of the framework, and 5 of the lakes (Erken, Greifensee, Lacawac, Mendota, and Montjoie) are not shown due to a short time period of available data.

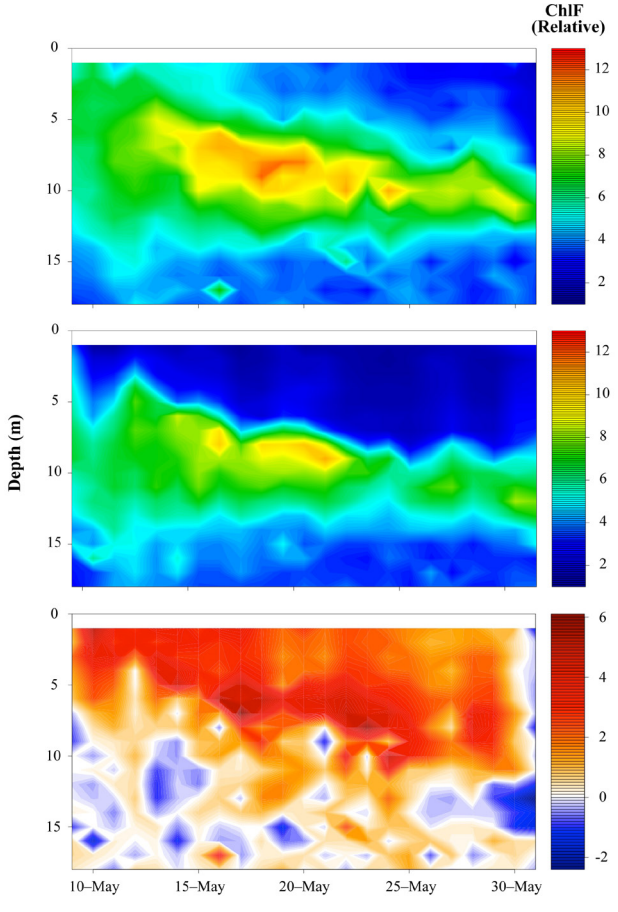

Fig. 2. Crystal Lake (WI, USA) midnight chlorophyll fluorescence (ChlF) profiles (top), noon ChlF profiles (middle), and the difference between midnight and noon ChlF (bottom) for 9–31 May 2014 to highlight the presence of sunlight-induced non-photochemical quenching and consequently lower ChlF in surface waters during the day compared to at night.

To assess the different temporal and vertical scales of variability in ChlF, daily vertical profiling buoy data from Lacawac were compared to high temporal but low vertical resolution data collected at 1 m and to high vertical but low temporal resolution data collected weekly using manual profiles. Midnight ChlF vertical profiles from 5 to 13 June 2014 were used. Missing data at 1 m on 9 and 11 June were filled with a linear interpolation procedure to facilitate visual comparisons. A daily average of the water column ChlF was also calculated for comparison with depth resolved vertical profiles. In addition, for each study lake, an annual and monthly average of the ratio of the mean of the water column ChlF to surface ChlF was calculated from nighttime profiles for the months with available data.

Physical control metrics

The 1% PAR depth, a proxy for the euphotic zone, and the depth of the metalimnion (top and bottom) for 3 lakes (Crystal, Montjoie, and Greifensee) were calculated. For Greifensee, linear interpolation was used to fill missing ChlF data to 0.1 m intervals over periods <2 d. A daily estimate of the 1% PAR depth was calculated from noon profiles or from the profile closest to noon between 1000 and 1600 h. Diffuse attenuation coefficients (K_d) for PAR were calculated using the Lambert-Beer equation from vertical profiles of downwelling irradiance (Kirk 1994):

$$K_{\mathrm{d}} = \frac{-\ln\left[\frac{E_d(z)}{\mathrm{E_d}(0)}\right]}{z} \quad (1)$$

where E_d (0) represents the irradiance immediately below the surface of the lake, and E_d (z) represents the irradiance at depth z. The euphotic depth ($Z_{1\%}$) was calculated from equation 1.

To estimate the daily upper and lower boundaries of the metalimnion, water temperature data from midnight profiles were binned to 0.5 m increments. Nighttime profiles were used to be consistent with the ChlF profiles and to avoid transient diurnal stratification effects, which can occasionally occur during midday on small lakes. The metalimnion was defined based on water density but corresponded approximately to the depths in the lake with a gradient >1 °C m^{-1} at temperatures ~20 °C (Wetzel 2001). The metalimnion depths were calculated using the rLakeAnalyzer package (Winslow et al. 2014) based on the methods in Read et al. (2011). All analyses were performed in R 3.1.1 (R Development Core Team 2015).

Results

SSCM were observed at some point during the seasonal time period in all lakes except 4 of the mesotrophic to eutrophic lakes (Bure, Rotoehu, Mendota, and Erken), of which 2 are polymictic (Bure and Rotoehu). Early season data were absent in Erken and Mendota, so possibly an SSCM was missed. As the season progressed, the SSCM peak typically increased in depth and became narrower in width. For oligotrophic lakes, the SSCM were more common and persistent throughout the entire season, whereas in the most eutrophic lakes, including Greifensee and Kinneret, an SSCM was present at the beginning of the time series, but the depth of the ChlF maximum moved to the surface waters shortly thereafter and remained there for the rest of season.

Profiling buoys and the PEG model

Overall, the eutrophic lakes showed better agreement with the PEG model than did the oligotrophic lakes (Fig. 3), although variability among lakes was high in the number, magnitude, and timing of the phytoplankton peaks. Three clear temporal peaks in phytoplankton were evident, including in spring, summer, and fall in Rotoehu and Bure (Fig. 3a and b), as presented in the PEG model. In Kinneret, only 2 well-defined peaks were present, followed by multiple small peaks (Fig. 3c). For the oligotrophic lakes, the PEG model hypothesized only 2 peaks in the spring/early summer and fall, with a prolonged clear-water phase in between (Sommer et al. 1986). Crystal showed the greatest similarity to the 2 peaks in the PEG model (Fig. 3d). Furnace and Ashokan exhibited multiple smaller seasonal peaks (Fig. 3e and f) and clearly differed from the PEG model.

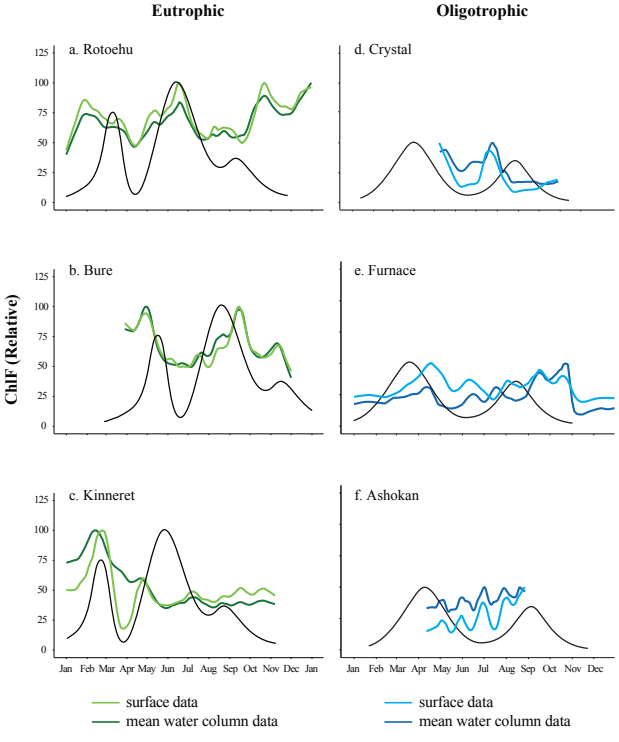

Fig. 3. Plankton Ecology Group (PEG) model of changes in phytoplankton biomass (black line from Sommer et al. 2012) overlaid on surface and mean water column midnight chlorophyll fluorescence (ChlF) data collected from profiling buoys for eutrophic and oligotrophic lakes. Lakes are arranged in order of increasing trophic status for eutrophic lakes (left) and oligotrophic lakes (right): (a) Rotoehu, (b) Bure, (c) Kinneret, (d) Crystal, (e) Furnace, (f) Ashokan.

With respect to the relative height of the seasonal peaks, the profiling buoy data in the eutrophic lakes rarely showed agreement with the PEG model. The spring peak was typically greater than or equal to the summer peak. Consistent with the PEG model, however, the fall peak was typically the lowest except in Rotoehu (Fig. 3a). Across the oligotrophic lakes, the fall peaks were all similar or greater in magnitude than any early-season peaks (Fig. 3d and f). The spring and fall peaks were similar in height in Crystal and Furnace (Fig. 3d and e), although in Crystal the second peak occurred in mid-summer rather than fall. Ashokan had several smaller peaks that increased progressively toward the fall (Fig. 3f).

Mean water column data from the eutrophic lakes showed the greatest agreement with the PEG model in relation to the timing of the phytoplankton peaks. In Kinneret, the spring peak and subsequent clear-water phase matched up well with the timing in the PEG model, but in Bure the spring peak occurred slightly earlier, and the summer peak occurred later than the PEG model (Fig. 3b and c). In Rotoehu, which does not freeze, the initial spring peak occurred earlier than hypothesized, but the summer peak lined up well (Fig. 3a). Among the oligotrophic lakes, the timing differed from the PEG model, with additional peaks present between the predicted bimodal pattern (Fig. 3d and f). Because of differences in the duration of ice cover and the absence of early spring data in some of the oligotrophic lakes, more data may be required to fully assess the timing of the peaks.

Surface profiling buoy data followed a similar pattern to the mean water column data in most of the lakes, especially in the eutrophic lakes. Mean water column data were consistently greater than the surface data in oligotrophic Ashokan and Crystal throughout the season, but for the remaining lakes they were more closely aligned except for a few time periods. In Kinneret and Crystal, the greatest difference between the mean water column and surface data occurred during the clear-water phase when the surface data followed the PEG model decline more closely, whereas the mean water column data remained

 DOI: 10.5268/IW-6.4.890

higher (Fig. 3c and d). Across the study lakes, the oligotrophic lakes, which all had a SSCM present during some or all of the time series, showed greater differences and complexity compared to the PEG model than for the eutrophic lakes, which only had SSCM present at certain time periods or not at all.

Scales of variability

The analysis comparing conventional sampling (i.e., manual profiles or single-depth sensors) with the higher resolution profiling buoy data revealed that high-frequency profiles were more effective at capturing short-term changes in phytoplankton dynamics that occur on a daily scale (Fig. 4). Hypothetical manual ChlF water column profiles taken 6 days apart in Lake Lacawac showed similar conditions with a ChlF maximum ~5 m on 6 June moving up to 3 m on 12 June. Between the manual profiles, the high-frequency data revealed a higher magnitude ChlF maximum at 3–6 m that was missed by the manual profiles. In addition, a single depth sensor moored at 1 m in the lake would have missed the peak in ChlF, and little change in the surface waters was observed. The daily water column average also did not capture the changes in vertical distribution of ChlF (Fig. 4).

The annual average ratio of mean water column ChlF to surface ChlF was close to 1, except for the most oligotrophic lakes (Table 3). The annual ratio ranged from 1.88 in highly oligotrophic Crystal to 0.80 in eutrophic Mendota, with the remaining lakes ranking mostly according to their trophic status. On a monthly scale, the ChlF ratio was highly variable. In some lakes, including Kinneret, the ratio was highest in the winter to spring months, whereas in other lakes such as Furnace and Bure, the difference between the full water column and the surface was often greater in the late summer and fall months (Table 3).

A closer examination of the patterns in Kinneret revealed a strong peak in the ChlF maximum from early March through April, which then sank dramatically, followed by a redevelopment of a surface bloom beginning around mid-May (Fig. 5). The ratio of mean water column ChlF to surface ChlF was highest in March (1.85) but otherwise ~1 for the rest of the time series (Table 3). For Furnace, a different pattern emerged, in which differences between the surface and the water column average were greatest in July (1.41) and October (1.34). The surface readings in Kinneret and Furnace were also highly variable, with occasional large daily peaks in early March in Kinneret and from September through November in Furnace (Fig. 5). In Crystal, a prominent SSCM during most of the time series caused the mean water column data to be greater than the surface data by as much as 2-fold from June through September (Fig. 5).

Physical control

A visual comparison of the seasonal changes in the physical control metrics in relation to ChlF maxima showed large variation across 3 lakes of differing trophic status—Crystal, Montjoie, and Greifensee—conceptualized into 2 scenarios. The euphotic depth, or the top of the metalimnion (i.e., bottom of the mixed layer), was often closely aligned to the depth of the ChlF maximum (Fig. 6). In the clearest lake, Crystal (top), the depth of the ChlF maximum was much greater than the metalimnion depths and corre-

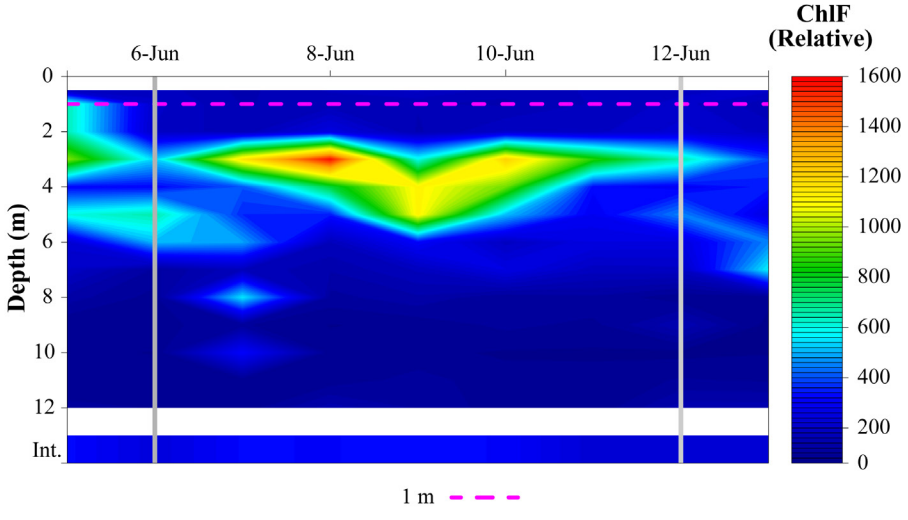

Fig. 4. Midnight chlorophyll fluorescence (ChlF) profiles from Lake Lacawac from 5–13 June 2014 showing subsurface ChlF dynamics captured by daily vertical profiles but would be missed by the more conventional less frequent vertical profiles (vertical gray lines) or single depth surface sensors on a buoy (horizontal hatched pink line). Blue bar at the bottom of figure represents daily mean ChlF for the entire water column, which also does not effectively capture the metalimnetic ChlF maximum.

Table 3. Monthly and annual ratio of the mean water column chlorophyll fluorescence (ChlF) to ChlF at the surface (depth range 0–2 m) for the study lakes arranged according to lake trophic status in Table 1. Ratios are calculated at an annual scale for the entire season and the specific months where data were present. Values of "na" represent months where no data were collected for that lake. The ratios indicate whether the average chlorophyll concentration as estimated by ChlF in the water column is greater (ratio > 1) or less (ratio < 1) than ChlF estimated from surface readings alone.

Lake	Annual	Jan	Feb	Mar	Apr	May	Jun	Jul	Aug	Sep	Oct	Nov	Dec
Lacawac	1.59	na	na	na	na	na	1.82	1.67	0.91	na	na	na	na
Crystal	1.88	na	na	na	na	1.41	2.42	2.02	2.01	2.02	1.22	na	na
Montjoie	1.07	na	na	na	na	na	0.91	1.14	1.05	na	na	na	na
Furnace	0.95	0.99	1.10	0.99	0.74	0.64	0.78	1.41	0.78	1.15	1.34	0.67	0.79
Ashokan	1.34	na	na	na	1.38	1.37	1.18	1.22	0.89	na	na	na	na
Erken	0.98	na	na	na	na	na	na	1.00	0.91	0.99	1.03	na	na
Rotoehu	1.08	1.07	1.15	1.07	1.17	1.06	1.08	1.04	1.03	1.05	1.10	1.05	1.03
Bure	1.09	na	na	na	1.06	1.06	1.08	1.08	1.29	1.09	1.05	1.05	1.05
Greifensee	0.82	na	na	na	na	na	0.98	0.95	0.68	0.64	na	na	na
Mendota	0.80	na	na	na	na	na	0.58	0.83	0.81	na	na	na	na
Kinneret	0.89	1.15	0.96	1.85	1.06	0.71	0.70	0.64	0.61	0.54	0.56	na	na

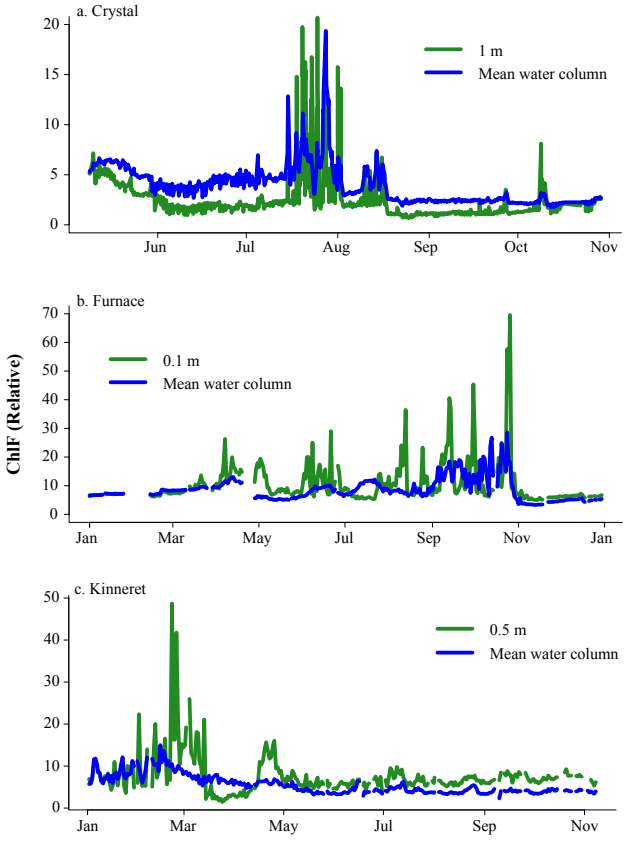

Fig. 5. Comparison of nighttime chlorophyll fluorescence (ChlF) data collected with a profiling buoy at the lake surface (green line) and averaged over the full water column (blue line) for (a) oligotrophic Crystal, (b) oligotrophic-dystrophic Furnace, and (c) eutrophic Kinneret.

sponded instead fairly closely to the depth of the euphotic zone (Fig. 6). By contrast, for mesotrophic Montjoie (middle), the ChlF maximum was primarily between the upper and lower metalimnion depths and shallower than the depth of the euphotic zone (Fig. 6). In this lake, the light attenuation is largely controlled by relatively constant colored dissolved organic matter absorption (data not shown). For Greifensee (bottom), an SSCM was present at the beginning of the time series with 2 peaks evident in late July, but by August, ChlF was highest in the surface waters. Early in the season, the depth of the euphotic zone was greater than the depth of the top and bottom of the metalimnion but decreased dramatically around 15 July and became shallower than the top of the metalimnion. The shallowing of the euphotic zone coincided with a shift in the ChlF peak from the metalimnion into the eplimnion. As the depth of the metalimnion and euphotic zone deepened in the fall, and ChlF maximum subsequently moved deeper in the water column (Fig. 6).

Discussion

High-frequency profiling buoy data revealed that many critical aspects of phytoplankton vertical and temporal dynamics would not be captured with conventional sampling techniques based on weekly vertical profiles or high-frequency, single-depth sensors located in the epilimnion. Intense, short-lived subsurface ChlF maxima are often entirely missed with either of the 2 conventional sampling approaches. High-frequency mean water column ChlF data indicated that in 6 of 11 lakes, surface-only estimates of ChlF underestimated phytoplankton

 DOI: 10.5268/IW-6.4.890

abundance at an annual scale due to the presence of SSCM. The underestimation was most pronounced in the more oligotrophic lakes and ranged up to a nearly 2-fold difference. Even for the most eutrophic lake, Kinneret, an SSCM present for a brief period in the spring caused surface ChlF to underestimate water column ChlF for 2 months.

As a general framework, the PEG model provides a useful way to conceptualize seasonal phytoplankton dynamics, but it is most effective in lakes where the euphotic zone is shallower than the top of the metalimnion. Physical control of phytoplankton during the primary growing season was also proposed to be of minimal importance in the PEG model, but here we suggest that the seasonal deepening of the mixed layer and euphotic zone likely play an important role, along with other biological factors including zooplankton grazing (Longhurst 1976, Williamson et al. 1996, Pilati and Wurtsbaugh 2003) and nutrient availability (Saros et al. 2005) in structuring the SSCM. Our results show that an exclusive focus on epilimnetic samples or less frequent vertical profiles could potentially miss an important component of total ecosystem productivity that occurs in SSCM layers in many lakes.

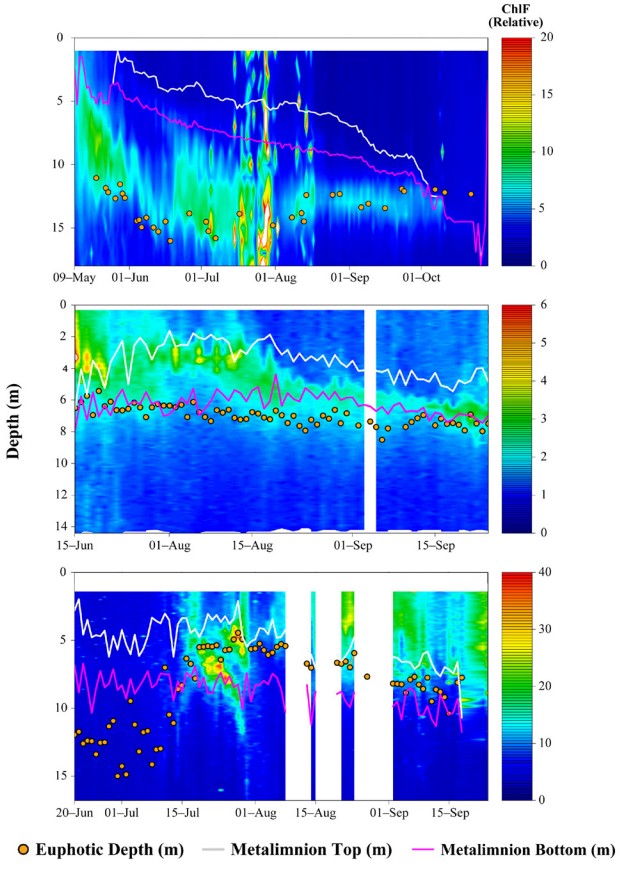

Fig. 6. Depth vs. time isopleths of midnight chlorophyll fluorescence (ChlF) data in Crystal (top), Montjoie (middle), and Greifensee (bottom). Lines indicate the boundaries of the metalimnion top (white line), metalimnion bottom (pink line), and euphotic depth (1% PAR, orange points).

The lake that showed the greatest similarity to the eutrophic PEG model was mesotrophic, polymictic Bure, in which a lack of consistent thermal stratification prevented the development of a SSCM. For the thermally stratified mesotrophic and eutrophic lakes, the difference in ChlF between the epilimnion and the water column was greatest in the spring or early summer when SSCM were more likely due to deeper light penetration and a shallower epilimnion, as has been shown for 5 New Zealand lakes (Hamilton et al. 2010, Simmonds et al. 2015). As the growing season progressed, however, the mixed layer depth deepened and the euphotic zone became shallower, confining the phytoplankton to the mixed, well-lit surface waters. During this period, surface ChlF readings and the PEG model yielded a good assessment of phytoplankton dynamics, and full water column profiles were similar to the surface data or slightly underestimated ChlF.

Differences between mean water column ChlF and surface ChlF data were clearly revealed in Kinneret and Crystal, in which the magnitude of the clear-water phase decline in phytoplankton would have been overestimated if only surface data were used. The clear-water phase is one of the most important phenological events for the seasonal dynamics of phytoplankton (Lampert et al. 1986), but the decline of phytoplankton biomass may be less than hypothesized because high-frequency full water column sampling was able to capture a deepening of the ChlF maximum that would have been missed with only epilimnetic sampling. Additionally, the relative sizes of the peaks for the lakes in this study were inconsistent with the PEG model. The spring peak was often equal to or greater in magnitude than the summer or fall peak, potentially due to the inclusion of SSCM, with the exception being Ashokan and Furnace. For these lakes, the increase in the number and magnitude of the peaks later in the season may have been due to weaker stratification in the reservoir, or in Furnace, the influx of brackish water during high tides may cause SSCM to develop and breakdown frequently (E. de Eyto, Marine Institute, unpublished data).

Latitudinal and climatic differences may explain the altered timing of the ChlF peaks between the study lakes and the PEG model because the original framework developed almost 30 years ago was based primarily on temperate ice-covered lakes, except for 2 subtropical African lakes (Sommer et al. 1986). The study lakes in this dataset covered a range of latitudes, including 2 subtropical lakes and 3 high northern latitude lakes, so differences in the magnitude and timing of the peaks could potentially be due to the inclusion of SSCM in the mean water column data, deviations in length of the

growing season, or other climatic factors. Under predicted future climate change scenarios, the PEG model was recently revisited, and projections were made for the effects of increased temperature and precipitation on phytoplankton dynamics in lakes across a range of latitudes (De Senerpont Domis et al. 2013). In high northern latitude lakes, increases in temperature are likely to lengthen the growing season, which will prolong seasonal phytoplankton production. Additional nutrient inputs to these lakes from higher rates of runoff or internal nutrient loading from anoxic sediments were shown to increase the magnitude of the biomass peaks. Subtropical lakes, which were specifically separated into their own model, are expected to see increases in precipitation intensity that increase runoff of terrestrial dissolved organic matter and nutrients. Thus, these lakes are predicted to experience higher fluctuations in phytoplankton abundance and altered species composition that may greatly affect the overall seasonal patterns (De Senerpont Domis et al. 2013). The role of SSCM and the influence of physical factors during the growing season, however, were still largely neglected in this revised model.

An important challenge with both conventional and profiling buoy sampling approaches is that phytoplankton show strong patterns of horizontal patchiness in both space and time (Hillmer et al. 2008, Durham et al. 2013). The dynamics of these rapidly changing surface bloom patterns can be more easily visualized from satellite images (Gregg et al. 2005, Odermatt et al. 2012, Lesht et al. 2013) but are not captured by stationary sampling techniques. What appear to be strong temporal variations in phytoplankton dynamics captured by stationary sampling methods could potentially be due to the advection or wind-driven movements of water masses with higher phytoplankton densities rather than singular blooms and declines in phytoplankton abundance at one point in space (Durham and Stocker 2012, Durham et al. 2013). This phenomenon may account for, at least in part, the large number of phytoplankton peaks observed throughout the summer in many of the study lakes. An additional challenge is that ChlF was used as a proxy of phytoplankton biomass, an approach with inherent limitations because phytoplankton biomass peaks are not necessarily at the same location as peaks in chlorophyll fluorescence (Cullen 1982, Fennel and Boss 2003). ChlF remains a commonly accepted method to measure phytoplankton *in situ*, however, and represents a useful way to assess phytoplankton vertical dynamics at short time scales (Huot and Babin 2010). When examining SSCM for future studies, simultaneous profiles of biomass measurements with ChlF are recommended to inform if the fluorescence data match biomass estimates.

An event that may impede the unambiguous interpretation of deep ChlF as a proxy for phytoplankton biomass is the occurrence of metalimnetic phototrophic bacteria blooms, a phenomenon in lakes that causes a sulfide enriched hypolimnion to develop (Van Gemerden and Mas 1995). As such, favorable conditions for phototropic bacteria do exist in 2 eutrophic lakes in this study. Because *in situ* profiling with common fluorescence sensors does not allow chlorophyll and bacteriochlorophyll to be distinguished (Rimmer et al. 2008), additional information is required to correctly interpret the SSCM. In Kinneret, metalimnetic blooms of green sulfur bacteria occur during early summer and fall depending on the light conditions and the chemical stratification process (Eckert et al. 1990), but the dataset used in this study did not exhibit elevated ChlF below the thermocline during that time. The increased metalimnetic ChlF in Greifensee during July–August is unlikely to be the result of a phototrophic bacteria bloom because sulfide accumulation in this lake was shown to be restricted to late fall (Sigg et al. 1991).

The differences between the seasonal patterns observed here and those hypothesized by the PEG model are likely due to the ability of frequent, full vertical profiles to more effectively capture subsurface phytoplankton dynamics in some lakes. Over the season, the peaks in ChlF occurred progressively deeper in the water column, making it likely that epilimnetic sampling would be less representative of water column ChlF as the summer progressed. Drivers of the SSCM include physical changes in thermal structure and light availability in the water column as well as grazing pressure and nutrient availability, but the latter 2 are not addressed in this study, which focused instead on physical drivers.

Physical control factors were hypothesized in the original PEG model to have minimal influence on phytoplankton dynamics during the primary growing season (Sommer et al. 1986, 2012). Without data on nutrients and zooplankton dynamics, we cannot compare the relative strength of biological versus physical control on phytoplankton vertical distributions, but a visual comparison of critical physical habitat boundaries with ChlF dynamics suggests that physical control plays an important role in structuring the depth of ChlF maxima. Previous studies established that thermal stratification is an important precursor to the development of a SSCM (Hamilton et al. 2010, Jobin and Beisner 2014, Cullen 2015). In strongly oligotrophic lakes, the 1% PAR depth was closely related to the depth of the SSCM, which was located in the hypolimnion, well below the bottom of the metalimnion. Hypolimnetic SSCM correlated with the 1% PAR depth have also been previously observed in other highly transparent lakes, including Lake Tahoe and Crater Lake (Abbott et al. 1984, Fennel and Boss 2003). For the meso-oligotrophic and eutrophic lakes, variations in the depth of ChlF maxima were related to the depth of

 DOI: 10.5268/IW-6.4.890

the top of the metalimnion relative to the euphotic depth.

These close associations between the physical habitat boundaries and the SSCM highlight the need for a new conceptual framework that more explicitly includes abiotic metrics when determining the likelihood of SSCM formation in lakes. When the euphotic depth is greater than the metalimnion top, an SSCM will be more likely to form, whereas in lakes where the euphotic depth is less than the top of the metalimnion, the chlorophyll maximum will be confined to the epilimnion (Fig. 7). Although data from only 3 lakes were examined in detail, SSCM in 2 of the lakes were present for the entire time period, and the euphotic depth was consistently greater than the metalimnion top in Crystal and Montjoie. Greifensee provided a unique example of both scenarios because an SSCM was present in mid-July, but by mid-August the mixed layer depth was equal to the euphotic depth, so the SSCM was likely entrained into the surface waters.

Because significant dynamics occur outside the epilimnion observed by surface sensors, overall, profiling buoys are likely to be most useful in lakes where an SSCM can form (Fig. 7). This phenomenon may occur throughout the entire stratified season in high-transparency lakes, only at certain time periods in lower transparency lakes (e.g. Simmonds et al. 2015), or not at all in polymictic lakes. Thus, we suggest an extension to the PEG model in lakes where the euphotic depth extends below the mixed layer that explicitly includes the full water column and any SSCM present. SSCM may alter seasonal phytoplankton dynamics primarily through a reduction in the strength of the CWP decline and higher biomass during the spring and potentially summer peak as well. Other factors including nutrient limitation, differences in phytoplankton community composition, and zooplankton dynamics also influence the location and strength of the chlorophyll maximum (Beisner and Longhi 2013), so coupling higher resolution biological data, such as scanning flow-cytometry with physical data, is still needed to more fully understand phytoplankton dynamics (Pomati et al. 2011). SSCM consisting of some species of cyanobacteria (i.e., *Planktothrix rubescens*) and flagellates may be missed with ChlF sensors because their pigments are not detected, so combining microscopic and fluorimetric methods can provide important new insights into niche separation of different phytoplankton species (Selmeczy et al. 2015, Simmonds et al. 2015).

Automated profiling buoys with high-frequency sensors are capable of improving the understanding of complex lake processes, but the benefits of collecting higher spatial and temporal resolution data must be weighed against the financial and technical investment required to collect these data. Profiling buoys are expensive to operate and maintain, and the high cost of sensors, combined with a winch system, potentially make the applicability of these systems to a large number of lakes somewhat limited. On the technical side, differences in the stabilization time of different sensors require the profiling speed to be matched carefully, and mechanical problems can be common with the winch when repeatedly raising and lowering a suite of sensors.

Despite some limitations associated with profiling buoys, the ability to simultaneously collect automated high temporal and vertical resolution data on biological, chemical, and physical parameters in lakes will allow many more mechanistic links to be made between different ecosystem level processes. In a recent study on 3 lakes in Denmark, profiling buoy data captured vertical differences in metabolism, which improved the reliability of

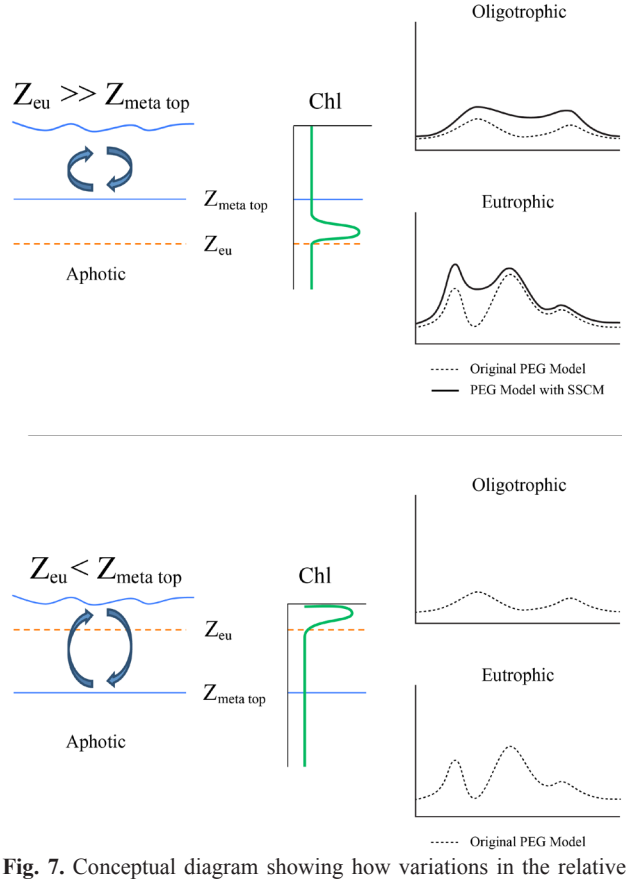

Fig. 7. Conceptual diagram showing how variations in the relative depths of the euphotic zone and the top of the metalimnion alter the seasonal patterns of phytoplankton biomass as proposed by the PEG model. In lakes where the euphotic zone (using 1% PAR depth as a proxy) is deeper than the top of the metalimnion, subsurface chlorophyll maxima (SSCM) will be more likely due to greater light penetration and a stable, thermally stratified water column. In these lakes, a modified version of the original PEG model is proposed with an explicit inclusion of the full water column and SSCM. When the euphotic zone is shallower than the top of the metalimnion, SSCM are unlikely, and the chlorophyll maximum will be confined to the surface waters. For these lakes, the original PEG model approximates the seasonal phytoplankton patterns well.

whole-lake net ecosystem production estimates (Obrador et al. 2014). When the euphotic depth was greater than the mixed layer depth (SSCM likely; see Fig. 7), areal metabolic estimates of gross primary production and respiration based on surface measurements deviated 60% and 80%, respectively, from depth-integrated estimates.

Comparisons across a range of different lakes with high-frequency temporal and vertical data are necessary to understand complex process including the formation, development, and breakdown of SSCM. The PEG model remains as a useful conceptual understanding of seasonal phytoplankton dynamics, but in lakes with an SSCM, it may underestimate the depth distribution, complexity, and abundance of phytoplankton, particularly during the clear water phase. We suggest an extension of the PEG model by incorporating full vertical water column phytoplankton dynamics as well as the physical control of SSCM during the growing season. Profiling buoys are useful tools for capturing phytoplankton dynamics, particularly in lakes or at certain time periods when the euphotic depth is greater than the mixed layer depth and surface sampling alone or infrequent manual profiles might miss short-term dynamics. Further experimental research on the contribution of these subsurface layers to total ecosystem productivity, and studies using a more quantitative approach to explicitly test for the influence of physical drivers on the depth and magnitude of the ChlF maxima in lakes of varying trophic status are needed. A full understanding of the biological and physical drivers of SSCM formation and their influence on lake ecosystem processes is still lacking, but high-resolution temporal and vertical data on phytoplankton dynamics have the potential to create critical new insights into important processes ranging from food web dynamics to lake metabolism and carbon cycling.

Acknowledgements

We thank Erin Overholt and Aaron Hebbeler for assistance in the lab and field. Special thanks go to Levyn Bürki and Colin Smith for database curation and to John Swain for figure layout assistance. For the Lacawac profiling buoy, we acknowledge the assistance of Bruce Hargreaves and Fondriest Environmental, Inc., who were instrumental in aiding with the design and construction. We also thank Lacawac Sanctuary Field Station for access to Lake Lacawac and their research facilities. The Lough Furnace profiling buoy is maintained through core Marine Institute funding and with the assistance of the field staff at the Burrishole research station. The Lake Rotoehu buoy is maintained with support from the Bay of Plenty Regional Council. We thank the New York City Department of Environmental Protection for sharing data from Ashokan Reservoir and the staff of the Upstate Freshwater Institute for assistance in collecting the data and maintaining the buoy monitoring program. This work was supported in part by GLEON student travel funding to JAB that allowed helpful discussions at the GLEON 16 meeting, as well as funding from Miami University and NSF DEB IGERT grant #0903560 to CEW. JSR was supported by the US Geological Survey Center for Integrated Data Analytics, and the Crystal Lake buoy was funded by NSF DEB grant #0822700 (North Temperate Lakes Long-Term Ecological Research, NTL-LTER). KCR received support from the NTL-LTER program. PAS was supported by the Danish Council for Independent Research Natural Sciences grant #10-085238. This manuscript benefited from helpful comments provided by David Hamilton and Christopher Dada. Any use of trade, firm, or product names is for descriptive purposes only and does not imply endorsement by the US Government.

References

Abbott ML, Denman KL, Powell T, Richerson PJ, Richards R, Goldman C. 1984. Mixing and the dynamics of the deep chlorophyll maximum in Lake Tahoe. Limnol Oceanogr. 29:862–878.

Barbiero RP, Tuchman ML. 2004. The deep chlorophyll maximum in Lake Superior. J Great Lakes Res. 30(Suppl 1):256–268.

Beisner BE, Longhi ML. 2013. Spatial overlap in lake phytoplankton: relations with environmental factors and consequences for diversity. Limnol Oceanogr. 58:1419–1430.

Brookes JD, Carey CC. 2011. Resilience to blooms. Science. 334:46–47.

Caron DA, Stauffer B, Moorthi S, Singh A, Batalin M, Graham EA, Hansen M, Kaiser WJ, Das J, Pereira A, et al. 2008. Macro- to fine-scale spatial and temporal distributions and dynamics of phytoplankton and their environmental driving forces in a small montane lake in southern California, USA. Limnol Oceanogr. 53:2333–2349.

Carpenter SR, Caraco NF, Correll DL, Howarth RW, Sharpley AN, Smith VH. 1998. Nonpoint pollution of surface waters with phosphorus and nitrogen. Ecol Appl. 8:559–568.

Cassina F, Dalton C, Dillane M, de Eyto E, Poole R, Sparber K. 2013. A multi-proxy palaeolimnological study to reconstruct the evolution of a coastal brackish lake (Lough Furnace, Ireland) during the late Holocene. Paleogeogr Paleoclimatol Paleoecol. 383:1–15.

Cullen JJ. 1982. The deep chlorophyll maximum: comparing vertical profiles of chlorophyll *a*. Can J Fish Aquat Sci. 39:791–803.

Cullen JJ. 2015. Subsurface chlorophyll maximum layers: enduring enigma or mystery solved? Ann Rev Mar Sci. 7:207–239.

De Senerpont Domis LN, Elser JJ, Gsell AS, Huszar VLM, Ibelings BW, Jeppesen E, Kosten S, Mooij WM, Roland F, Sommer U, et al. 2013. Plankton dynamics under different climatic conditions in space and time. Freshwater Biol. 58:463–482.

Dickey TD, Itsweire EC, Moline MA, Perry MJ. 2008. Introduction to

 DOI: 10.5268/IW-6.4.890

the Limnology and Oceanography Special Issue on autonomous and Lagrangian platforms and sensors (ALPS). Limnol Oceanogr. 53:2057–2061.

Dodds W, Bouska WW, Eitzmann JL, Pilger TJ, Pitts KL, Riley AJ, Schloesser JT, Thornbrugh DJ. 2009. Eutrophication of U.S. freshwaters: analysis of potential economic damages. Environ Sci Technol. 43:12–19.

Dröscher I, Patoine A, Finlay K, Leavitt PR. 2009. Climate control of the spring clear-water phase through the transfer of energy and mass to lakes. Limnol Oceanogr. 54:2469–2480.

Durham WM, Climent E, Barry M, De Lillo F, Boffetta G, Cencini M, Stocker R. 2013. Turbulence drives microscale patches of motile phytoplankton. Nat Commun. 4:2148. doi:10.1038/ncomms3148

Durham WM, Stocker R. 2012. Thin phytoplankton layers: characteristics, mechanisms, and consequences. Ann Rev Mar Sci. 4:177–207.

Eckert WY, Yacobi YZ, Trüper HG. 1990. A bloom of a brown phototrophic sulfur bacterium in Lake Kinneret: hydro-chemical aspects. Microb Ecol. 20:273–282.

Fee EJ. 1976. The vertical and seasonal distribution of chlorophyll in lakes of the Experimental Lakes Area, northwestern Ontario: implications for primary production estimates. Limnol Oceanogr. 21:767–783.

Fennel K, Boss E. 2003. Subsurface maxima of phytoplankton and chlorophyll: steady-state solutions from a simple model. Limnol Oceanogr. 48:1521–1534.

Francis TB, Schindler DE, Holtgrieve GW, Larson ER, Scheuerell MD, Semmens BX, Ward EJ. 2011. Habitat structure determines resource use by zooplankton in temperate lakes. Ecol Lett. 14:364–372.

Geider RJ, MacIntyre HL, Kana TM. 1998. A dynamic regulatory model of phytoplanktonic acclimation to light, nutrients, and temperature. Limnol Oceanogr. 43:679–694.

Gregg WW, Casey NW, McClain CR. 2005. Recent trends in global ocean chlorophyll. Geophys Res Lett. 32:L03606. doi:10.1029/2004GL021808

Grimm NB, Chapin FS, Bierwagen B, Gonzalez P, Groffman PM, Luo YQ, Melton F, Nadelhoffer K, Pairis A, Raymond PA, et al. 2013. The impacts of climate change on ecosystem structure and function. Front Ecol Environ. 11:474–482.

Hamilton DP, Carey CC, Arvola L, Arzberger P, Brewer C, Cole JJ, Gaiser E, Hanson PC, Ibelings BW, Jennings E, et al. 2015. A Global Lake Ecological Observatory Network (GLEON) for synthesizing high-frequency sensor data for validation of deterministic ecological models. Inland Waters. 5:49–56.

Hamilton DP, O'Brien KR, Burford MA, Brookes JD, McBride CG. 2010. Vertical distributions of chlorophyll in deep, warm monomictic lakes. Aquat Sci. 72:295–307.

Hayes NM, Vanni MJ, Horgan MJ, Renwick WH. 2015. Climate and land use interactively affect lake phytoplankton nutrient limitation status. Ecology. 96:392–402.

Hillmer I, van Reenen P, Imberger J, Zohary T. 2008. Phytoplankton patchiness and their role in the modelled productivity of a large, seasonally stratified lake. Ecol Model. 218:49–59.

Huisman J, Thi NNP, Karl DM, Sommeijer B. 2006. Reduced mixing generates oscillations and chaos in the oceanic deep chlorophyll maximum. Nature. 439:322–325.

Huot Y, Babin M. 2010. Overview of fluorescence protocols: theory, basic concepts, and practice. In: Sugget D, Borowitzka MA, Prasil O, editors. Chlorophyll *a* fluorescence in aquatic science: methods and applications. Heidelberg (Germany): Springer Netherlands. p. 31–74.

Jobin VO, Beisner BE. 2014. Deep chlorophyll maxima, spatial overlap and diversity in phytoplankton exposed to experimentally altered thermal stratification. J Plankton Res. 36:933–942.

Kirk JTO. 1994. Light and photosynthesis in aquatic ecosystems. New York (NY): Cambridge University Press.

Lampert W, Fleckner W, Rai H, Taylor BE. 1986. Phytoplankton control by grazing zooplankton: a study on the spring clear-water phase. Limnol Oceanogr. 31:478–490.

Lesht BM, Barbiero RP, Warren GJ. 2013. A band-algorithm for retrieving open-lake chlorophyll values from satellite observations of the Great Lakes. J Great Lakes Res. 39:138–152.

Longhurst AR. 1976. Interactions between zooplankton and phytoplankton profiles in the eastern tropical Pacific Ocean. Deep Sea Res. 23:729–754.

Malkin SY, Silsbe GM, Smith REH, Howell ET. 2012. A deep chlorophyll maximum nourishes benthic filter feeders in the coastal zone of a large clear lake. Limnol Oceanogr. 57:735–748.

Matthews B, Mazumder A. 2006. Habitat specialization and the exploitation of allochthonous carbon by zooplankton. Ecology. 87:2800–2812.

Mellard JP, Yoshiyama K, Litchman E, Klausmeier CA. 2011. The vertical distribution of phytoplankton in stratified water columns. J Theor Biol. 269:16–30.

Mignot A, Claustre H, Uitz J, Poteau A, D'Ortenzio F, Xing XG. 2014. Understanding the seasonal dynamics of phytoplankton biomass and the deep chlorophyll maximum in oligotrophic environments: a Bio-Argo float investigation. Global Biogeochem Cy. 28:856–876.

Moll RA, Stoermer EF. 1982. A hypothesis relating trophic status and subsurface chlorophyll maxima of lakes. Arch Hydrobiol. 94:425–440.

Obrador B, Staehr PA, Christensen JPC. 2014. Vertical patterns of metabolism in three contrasting stratified lakes. Limnol Oceanogr. 59:1228–1240.

Odermatt D, Pomati F, Pitarch J, Carpenter J, Kawka M, Schaepman M, Wüest A. 2012. MERIS observations of phytoplankton blooms in a stratified eutrophic lake. Remote Sens Environ. 126:232–239.

Pilati A, Wurtsbaugh WA. 2003. Importance of zooplankton for the persistence of a deep chlorophyll layer: a limnocorral experiment. Limnol Oceanogr. 48:249–260.

Pomati F, Jokela J, Simona M, Veronesi M, Ibelings BW. 2011. An automated platform for phytoplankton ecology and aquatic ecosystem monitoring. Environ Sci Technol. 45:9658–9665.

Prairie JC, Franks PJ, Jaffe JS, Doubell MJ, Yamazaki H. 2011. Physical and biological controls of vertical gradients in phytoplankton. Limnol Oceanogr-Fluid Environ. 1:75–90.

Proctor CW, Roesler CS. 2010. New insights on obtaining phytoplankton concentration and composition from *in situ* multispectral chlorophyll fluorescence. Limnol Oceanogr-Meth. 8:695–708.

R Development Core Team. 2015. R: a language and environment for statistical computing. Vienna (Austria): R Foundation for Statistical Computing.

Read JS, Hamilton DP, Jones ID, Muraoka K, Winslow LA, Kroiss R, Wu CH, Gaiser E. 2011. Derivation of lake mixing and stratification indices from high-resolution lake buoy data. Environ Model Software. 26:1325–1336.

Reynolds CS. 2006. The ecology of freshwater phytoplankton. New York (NY): Cambridge University Press.

Reynolds CS, Walsby AE. 1975. Water-blooms. Biol Rev. 50:437–481.

Rimmer A, Ostrovsky I, Yacobi YZ. 2008. Light availability for *Chlorobium phaeobacteroides* development in Lake Kinneret. J Plankton Res. 30:765–776.

Saros JE, Interlandi SJ, Doyle SA, Michel TJ, Williamson CE. 2005. Are the deep chlorophyll maxima in alpine lakes primarily induced by nutrient availability, not UV avoidance? Arct Antarct Alp Res. 37:557–563.

Selmeczy GB, Tapolczai K, Casper P, Krienitz L, Padisak J. 2015. Spatial- and niche segregation of DCM-forming cyanobacteria in Lake Stechlin (Germany). Hydrobiologia. 764:1–12.

Serra T, Borrego C, Quintana X, Calderer L, López R, Colomer J. 2009. Quantification of the effect of nonphotochemical quenching on the determination of *in vivo* Chl-*a* from phytoplankton along the water column of a freshwater reservoir. Photochem Photobiol. 85:321–331.

Sigg L, Johnson CA, Kuhn A. 1991. Redox conditions and alkalinity generation in a seasonally anoxic lake (Lake Greifen). Mar Chem. 36:9–26.

Simmonds B, Wood SA, Oezkundakci D, Hamilton DP. 2015. Phytoplankton succession and the formation of a deep chlorophyll maximum in a hypertrophic volcanic lake. Hydrobiologia. 745:297–312.

Sommer U, Adrian R, De Senerpont Domis L, Elser JJ, Gaedke U, Ibelings B, Jeppesen E, Lürling M, Molinero JC, Mooij WM, et al. 2012. Beyond the Plankton Ecology Group (PEG) model: mechanisms driving plankton succession. Annu Rev Ecol Evol S. 43:429–448.

Sommer U, Gliwicz ZM, Lampert W, Duncan A. 1986. The PEG-model of seasonal succession of planktonic events in fresh waters. Arch Hydrobiol. 106:433–471.

Staehr PA, Christensen JPA, Batt RD, Read JS. 2012. Ecosystem metabolism in a stratified lake. Limnol Oceanogr. 57:1317–1330.

Taranu ZE, Gregory-Eaves I, Leavitt PR, Bunting L, Buchaca T, Catalan J, Domaizon I, Guilizzoni P, Lami A, McGowan S, et al. 2015. Acceleration of cyanobacterial dominance in north temperate-subarctic lakes during the Anthropocene. Ecol Lett. 18:375–384.

Van Gemerden H, Mas J. 1995. Ecology of phototrophic sulfur bacteria. In: Blankenship RE, Madigan MT, Bauer CE, editors. Anoxygenic photosynthetic bacteria. Dordrecht (Netherlands): Kluwer Academic. p. 49–85.

Weathers K, Hanson P, Arzberger P, Brentrup JA, Brookes JD, Carey CC, Gaiser E, Hamilton DP, Ibelings BW, Istvanovics V, et al. 2013. The Global Lake Ecological Observatory Network (GLEON): the evolution of grassroots network science. Limnol Oceanogr B. 22:71–73.

Wetzel RG. 2001. Limnology, lake and river ecosystems. New York (NY): Academic Press.

White B, Matsumoto K. 2012. Causal mechanisms of the deep chlorophyll maximum in Lake Superior: a numerical modeling investigation. J Great Lakes Res. 38:504–513.

Williamson CE, De Lange HJ, Leech DM. 2007. Do zooplankton contribute to an ultraviolet clear-water phase in lakes? Limnol Oceanogr. 52:662–667.

Williamson CE, Sanders RW, Moeller RE, Stutzman PL. 1996. Utilization of subsurface food resources for zooplankton reproduction: implications for diel vertical migration theory. Limnol Oceanogr. 41:224–233.

Winslow LA, Read JS, Woolway R, Brentrup JA, Leach TH, Zwart JA. 2014. rLakeAnalyzer: Package for the analysis of lake physics. R Package version 14.

 DOI: 10.5268/IW-6.4.890